

Modeling future scenarios of light attenuation and potential seagrass success in a eutrophic estuary



Pilar del Barrio ^{a,*}, Neil K. Ganju ^b, Alfredo L. Aretxabaleta ^b, Melanie Hayn ^c,
Andrés García ^a, Robert W. Howarth ^c

^a Environmental Hydraulics Institute “IH Cantabria”, C/ Isabel Torres n°15, Parque Científico y Tecnológico de Cantabria, 39011 Santander, Spain

^b U.S. Geological Survey, Woods Hole Coastal and Marine Science Center, 384 Woods Hole Road, Woods Hole, MA 02543, USA

^c Department of Ecology and Evolutionary Biology, Cornell University, Ithaca, NY, USA

ARTICLE INFO

Article history:

Received 30 January 2014

Accepted 6 July 2014

Available online 11 July 2014

Keywords:

seagrass
model
eutrophication
light attenuation
nutrient loading
sea level rise

ABSTRACT

Estuarine eutrophication has led to numerous ecological changes, including loss of seagrass beds. One potential cause of these losses is a reduction in light availability due to increased attenuation by phytoplankton. Future sea level rise will also tend to reduce light penetration and modify seagrass habitat. In the present study, we integrate a spectral irradiance model into a biogeochemical model coupled to the Regional Ocean Model System (ROMS). It is linked to a bio-optical seagrass model to assess potential seagrass habitat in a eutrophic estuary under future nitrate loading and sea-level rise scenarios. The model was applied to West Falmouth Harbor, a shallow estuary located on Cape Cod (Massachusetts) where nitrate from groundwater has led to eutrophication and seagrass loss in landward portions of the estuary. Measurements of chlorophyll, turbidity, light attenuation, and seagrass coverage were used to assess the model accuracy. Mean chlorophyll based on uncalibrated in-situ fluorometry varied from $28 \mu\text{g L}^{-1}$ at the landward-most site to $6.5 \mu\text{g L}^{-1}$ at the seaward site, while light attenuation ranged from 0.86 to 0.45 m^{-1} . The model reproduced the spatial variability in chlorophyll and light attenuation with RMS errors of $3.72 \mu\text{g L}^{-1}$ and 0.07 m^{-1} respectively. Scenarios of future nitrate reduction and sea-level rise suggest an improvement in light climate in the landward basin with a 75% reduction in nitrate loading. This coupled model may be useful to assess habitat availability changes due to eutrophication and sediment resuspension and fully considers spatial variability on the tidal timescale.

© 2014 Elsevier Ltd. All rights reserved.

1. Introduction

Seagrass meadows are found in many coastal areas around the world and are regarded as key indicators of ecosystem health (Dennison et al., 1993). They are among the most productive plant communities, and represent one of the major sources of primary production in shallow waters worldwide (Hemminga and Duarte, 2000). These plants serve as a nursery for many species, providing habitat and food for a variety of marine organisms (Orth et al., 2006). They also trap nutrients, thereby improving water transparency and filtering substantial quantities of both N and P from estuarine waters, serving as a buffer between land-based pollution sources and adjacent estuaries (Nixon et al., 2001; Short and Short, 2004; McGlathery et al., 2007; Hayn et al., 2014). Consequently, the increasing loss of seagrass beds raises concern

because of a potential reduction in coastal ecosystem productivity, a decrease in water quality, and a decline in fishing resources. Additionally, in a report prepared for the European Union, Terrados and Borum (2004) estimate the value of ecosystem services provided by seagrasses as two orders of magnitude higher than productive agricultural lands.

Despite the ecological and economic value of seagrass meadows, their disappearance has accelerated in the last decades (Short and Wyllie-Echeverria, 1996; Waycott et al., 2009). The causes of decline range from natural disturbances (e.g., storms) to anthropogenic pressures (e.g., nutrient loading). In temperate estuaries, one of the dominant factors for seagrass loss is eutrophication (Short and Neckles, 1999; Orth et al., 2006). In eutrophic waters, there is an overabundance of nutrients that leads to phytoplankton blooms, an increase in epiphytes growing on seagrass tissues, and subsequent light reduction (Burkholder et al., 2007). This reduction can impede seagrass growth and its ability to assimilate nitrogen, as they are vascular benthic autotrophs that require clear water and high levels of Photosynthetically Active Radiation (PAR). In fact,

* Corresponding author.

E-mail address: p.delbarrio@gmail.com (P. del Barrio).

minimum light requirements of seagrasses (2–37% of surface irradiance, SI) are much higher than those of macroalgae and phytoplankton (about 1–3% of SI) (Dennison et al., 1993; Lee et al., 2007). Therefore, seagrass photosynthesis, and thereby their growth, survival, and depth distribution, are directly linked to PAR reaching the plant surface (Cabello-Pasini et al., 2003). The spatial variation in light availability of eutrophic estuaries can cause changes in the spatial distribution of seagrass on the order of meters. Another aspect that should be taken into account is that the allocation and abundance of seagrasses have changed over evolutionary time in response to sea-level rise (SLR) (Orth et al., 2006). In areas where the tidal range increases, plants at the lower edge of the bed will receive less light at high tide, which increases plant stress, reduces photosynthesis, and therefore decreases the growth and survival of the vegetation (Short and Neckles, 1999; Titus et al., 2009). The complexity and variability of eutrophic estuaries with seagrass meadows highlights the need for a spatially explicit model that can resolve spatial distributions of chlorophyll, turbidity, colored dissolved organic matter (CDOM), and ultimately light attenuation. There are relatively few coupled hydrodynamic-light models that calculate light attenuation as a function of different attenuating substances apart from chlorophyll and water (Everett et al., 2007; Hipsey and Hamilton, 2008), and even fewer take into account spectral underwater irradiance (Bissett et al., 1999a, 1999b).

In the present study, we develop a new tool to assess the evolution of seagrass communities under future nitrate loading and sea-level rise scenarios using a three-dimensional circulation model (Regional Ocean Model System, ROMS) coupled to a Nutrient Phytoplankton Zooplankton Detritus (NPZD) eutrophication model (Fennel et al., 2006), where we have integrated a spectral light attenuation formulation (Gallegos et al., 2011). We describe the model and the linkage of this tool with a benthic seagrass model (Zimmerman, 2003), which calculates seagrass distribution. We

apply the model to West Falmouth Harbor, a temperate estuary where seagrass has considerably diminished in recent years in the more nitrogen-polluted inner reaches (Howarth et al., 2014). In the sections that follow we describe: 1) general features of West Falmouth Harbor, 2) the observational methods and results, 3) the numerical model and skill assessment, and 4) future scenarios of nitrate loading and sea-level rise. Finally, we discuss the utility and limitations of the approach and future directions.

2. Site description

West Falmouth Harbor is a eutrophic groundwater-fed estuary situated on the western shore of upper Cape Cod, Massachusetts, USA (Fig. 1). Tidal range at the harbor entrance is 1.9 m during spring tides and 0.7 m during neap tides (Ganju et al., 2012). The average depth is approximately 1 m, the surface area is 0.7 km² and the flushing rate is between 1 and 2 days. The harbor is connected to Buzzards Bay and ultimately the Atlantic Ocean through a 3 m deep, 150 m wide channel constrained by rock jetties on both sides (Ganju et al., 2012). The harbor is comprised of different sub-embayments (Outer Harbor, South Cove, and Snug Harbor). The presence of perennial eelgrass (*Zostera marina*), fish, and shellfish communities in the Harbor is particularly important from a habitat perspective. However, Costello and Kenworthy (2011) showed that there has been an ecologically significant alteration of eelgrass distribution in West Falmouth Harbor within the past decades. In 1979, eelgrass meadows were found throughout the harbor, with beds in the Outer Harbor, South Cove, and Snug Harbor (Costa, 1988). At present, these meadows have been lost from the landward basins, and eelgrass beds are only found in the Outer Harbor. In Snug Harbor, eelgrass beds died off as of mid summer of 2010, and grasses present during the previous several seasons had very high epiphyte loads on their blades and showed signs of considerable physiological stress (Howarth et al., 2014). The estimated

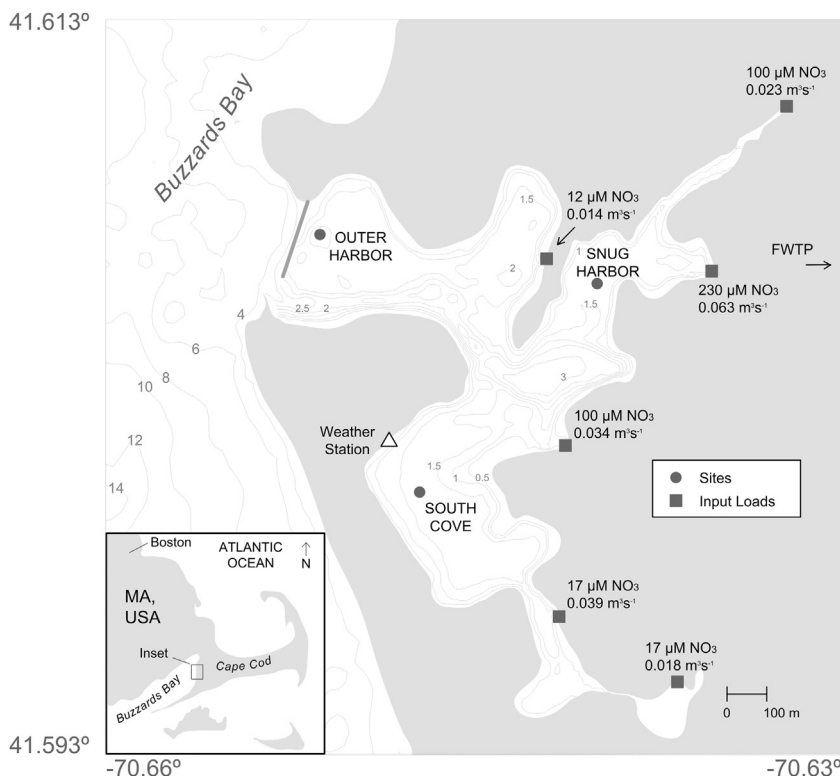


Fig. 1. West Falmouth Harbor, site locations and average summer input loads.

total area covered by seagrass was of 16.8 ha in 2010 (Hayn, 2012). In 2012, the seagrass area was reduced to 14.4 ha and no eelgrass beds were present in Snug Harbor. This pattern of eelgrass loss from the landward portions of the Harbor expanding toward the seaward regions is due to the excess nitrate loading to the harbor, which has contributed to eutrophication and associated processes such as light attenuation in the water column (Hayn et al., 2014; Howarth et al., 2014). This high nitrate load comes mainly from groundwater which naturally flows from the Sagamore lens of the Cape Cod aquifer; nitrate loads are high due to input from the Town of Falmouth Wastewater Treatment Plant (FWTP). The FWTP was constructed in the mid 1980's and is located landward of the Harbor, at a distance of 1 km east, with an average elevation of 30 m above sea level (Howes et al., 2006). Since 2005, nitrate input to groundwater from the FWTP has been substantially reduced due to an improvement in the sewage treatment. Nevertheless, given the groundwater travel time between the FWTP and West Falmouth Harbor (up to 10 years) (Kroeger et al., 2006), the effects of the nitrate loading reduction were still not apparent as of 2012 (Hayn et al., 2014). Moreover, surveys indicate that both the inner and outer basins would be capable of supporting eelgrass when the watershed nitrogen loading rates reached the levels of 1979–1985 (Howes et al., 2006). Therefore, it is thought that lowering nitrogen inputs to this system should provide the possibility of recovering seagrass communities and benthic habitats.

3. Observational methods

We deployed instrumentation in West Falmouth Harbor to measure meteorological, hydrodynamic, water quality, and light conditions during summer 2012 (Fig. 1). Meteorological data were measured at 1 min intervals by an Onset weather station from 28 June 2012 to 11 September 2012. Parameters included wind direction, wind speed, atmospheric pressure, relative humidity, shortwave radiation, PAR, and air temperature. The subaqueous instrument platform consisted of a Nortek Aquadopp ADCP (water velocity), a SeaBird SeaCat (pressure), a YSI 6600 multisonde (salinity, temperature, chlorophyll, turbidity, dissolved oxygen), and a pair of WetLabs ECO-PARSB sensors (PAR). All sensors were located 0.3 mab except for the upper PAR sensor located at 0.8 mab. The PAR sensors were equipped with wipers to prevent bio-fouling. The chlorophyll-a values were obtained by a YSI 6025 sensor located in the YSI 6600 multisonde. This sensor uses a light source with a peak wavelength of 470 nm which provokes the chlorophyll emission of light between 650 and 700 nm (fluorescence). The output of the sensor is automatically processed via the sonde software, which provides the chlorophyll ($\mu\text{g/L}$) readings. Here, we are reporting data as read from the multisonde sensor without any modification from external calibration. Some degree of fluorescence from other substances seems likely, especially during the last deployment of the sonde, given the somewhat lower values of chlorophyll measured in West Falmouth Harbor by extraction of filtered samples (Howarth et al., 2014). Measurements were collected at 5 min intervals from 3 to 19 July 2012 in Outer Harbor, from 19 July 2012 to 9 August 2012 in South Cove, and from 9 to 27 August 2012 in Snug Harbor. Due to the fact that no large intra-seasonal changes were observed between July and August during a previous field survey in 2010 (Ganju et al., 2011), the data collected in each location were considered representative of the season. Following Gallegos et al. (2011), we calculated the diffuse attenuation coefficient of downward propagating irradiance, K_d , as:

$$K_d = -\frac{1}{z} \ln \left(\frac{\text{PAR}_{\text{lower}}}{\text{PAR}_{\text{upper}}} \right) \quad (1)$$

where K_d is the light attenuation coefficient, z is the distance between the two sensors (0.5 m), $\text{PAR}_{\text{lower}}$ and $\text{PAR}_{\text{upper}}$ are the PAR measurements near the bottom and just below the water surface respectively during daylight.

To determine the areal extent of seagrass beds in West Falmouth Harbor we conducted surveys during early June 2012, using side scan sonar. We used an EdgeTech, Inc. 4125 towfish and EdgeTech Discover software to collect acoustic data at 900 and 1250 kHz along survey transects spaced to provide 200% bottom coverage in the survey area, and horizontal positions were provided by a Trimble AgGPS 132 with U.S.Coast Guard beacon differential corrections. We pre-processed the data in Chesapeake Technology Inc. SonarWiz5 to adjust for signal attenuation through the water, georeference the data, and export georeferenced imagery to ArcGIS 10.1 for classification. We manually delineated the seagrass beds in ArcGIS after examining ground-truthed locations to calibrate our image interpretation, and verified the final extent by surveying a random set of locations using a combination of surface and underwater observational techniques. Groundwater fluxes and associated nitrate concentrations (Fig. 1) were obtained in previous studies (Kroeger et al., 2006; Ganju et al., 2012; Hayn et al., 2014).

4. Observational results

Mean values of water column properties (temperature, salinity, pH, dissolved oxygen and turbidity) were overall spatially similar except for chlorophyll-a, which was highest at site Snug (Table 1). Fluorescence measurements suggested more eutrophication at landward ends of the harbor, with a mean uncalibrated chlorophyll value of $28 \mu\text{g L}^{-1}$, whereas in the outer harbor the mean uncalibrated chlorophyll concentration was $6.5 \mu\text{g L}^{-1}$. Accordingly, site Snug demonstrated considerably lower PAR values than site Outer (Table 2). PAR data from site South were not obtained due to instrument malfunction. The mean diffuse light attenuation coefficient K_d was 0.45 m^{-1} at site Outer and 0.86 m^{-1} at site Snug. Statistical distribution of chlorophyll measurements and K_d between the two sites confirms that the larger light attenuation coefficient present at site Snug is consistent with elevated chlorophyll-a concentration (Fig. 2). Prior measurements showed that CDOM is spatially uniform and relatively low in West Falmouth Harbor (absorbance at $440 \text{ nm} < 0.01 \text{ m}^{-1}$; M. Hayn, pers. comm.). These measurements also indicate that turbidity is relatively low with minimal spatial differences. Therefore there is a strong relationship between eutrophication (and ensuing chlorophyll-a levels) and light attenuation in the study area.

5. Model description

We integrated a spectral irradiance model (Gallegos et al., 2011) into an existing NPZD-biogeochemical model (Fennel et al., 2006)

Table 1
Mean values and standard deviation (Std) of measurements.

Field measurement	Units	Mean \pm Std		
		Outer	Snug	South
Chlorophyll-a	μgL^{-1}	6.46 ± 2.75	27.50 ± 9.90	10.22 ± 9.26
Turbidity	NTU	N/A*	4.26 ± 1.49	3.41 ± 1.39
Temperature	$^{\circ}\text{C}$	24.64 ± 0.84	25.84 ± 0.91	24.37 ± 0.81
Salinity	psu	30.94 ± 0.31	29.74 ± 0.65	30.51 ± 0.56
pH	—	8.01 ± 0.10	8.06 ± 0.49	7.97 ± 0.32
Dissolved oxygen	mgL^{-1}	7.17 ± 1.17	7.54 ± 1.44	6.75 ± 1.22

* Turbidity at site Outer was compromised by reflective copper tape (for anti-fouling) accidentally placed near the optical window. The tape tarnished within two weeks and did not affect subsequent measurements at sites Snug or South.

Table 2
Mean values, standard deviation (Std) and percentile 84 of measured optical data during daylight hours.

Field measurement	Units	Mean \pm Std		Percentile 84	
		Outer	Snug	Outer	Snug
PAR _{upper}	$\mu\text{E}/\text{m}^2\text{s}$	504 \pm 387	301 \pm 300	945	545
PAR _{lower}	$\mu\text{E}/\text{m}^2\text{s}$	416 \pm 327	198 \pm 209	795	363

to compute the spectral penetration of PAR through the water column. The coupled optical-biogeochemical model uses the PAR from the irradiance model to calculate phytoplankton growth. This model was integrated in the ROMS 3D circulation model (Haidvogel et al., 2008) that simulates the three-dimensional hydrodynamics. The computed PAR and K_d are provided to a bio-optical model (Zimmerman, 2003) that calculates the seagrass carbon balance under the estimated light climate (Fig. 3). The carbon balance allows the prediction of seagrass presence/absence and its potential survival. The capabilities of the linkage of these models provide an integral description of the physical, optical, and biological dynamics of the estuarine water column. This allows us to define a success criterion for assessing seagrass future evolution in a eutrophic estuarine system, based on light climate alone. In this section, we present a brief description of the main processes of each different model, although further information can be found in their respective references.

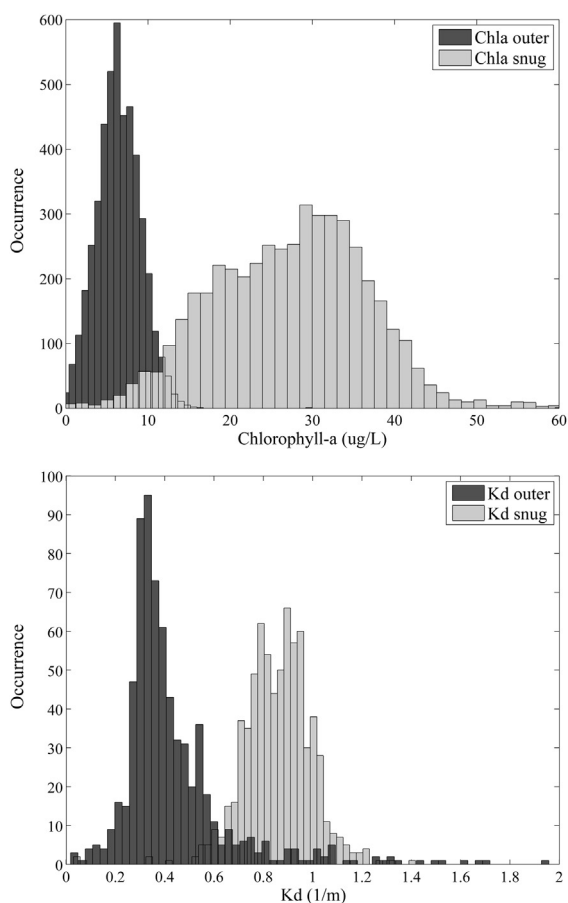


Fig. 2. Chlorophyll and K_d field data histograms in Outer and Snug Harbors. Data collected from sensors deployed during summer 2012 with a 5 min sampling interval.

5.1. Physical model

The circulation model used is the Regional Ocean Modeling System (ROMS) (Marchesiello et al., 2003; Haidvogel et al., 2008). ROMS is a three-dimensional, free-surface, terrain-following numerical model that solves the Reynolds-averaged Navier–Stokes equations using the hydrostatic and Boussinesq assumptions (Haidvogel et al., 2008).

In the physical configuration adopted, the outer domain is 2 km in the north-south direction centered on 41.6° latitude and 1.5 km in the east-west direction centered on -70.64° longitude (Fig. 1) and includes the entire West Falmouth Harbor estuarine system. The horizontal grid spacing is 10 m (150x200 grid points). The grid has 10 vertical levels using an evenly spaced vertical stretching. The spatial discretization of such a model allows for the representation of the spatial heterogeneity of the estuary in terms of light climate.

The model was forced at the western boundary (Fig. 1) with tidal free surface elevation, velocity, salinity and temperature. Additionally, the atmospheric forcing included wind velocities, atmospheric pressure, shortwave radiation, surface air temperature and relative humidity. These data were obtained from the weather station located in the study area (Fig. 1) and were applied as surface forcing in the entire computational domain. Groundwater fluxes, nitrogen loads, and fresh water temperature were given to the model as point sources. These fluxes were quantified from velocity and salinity measurements and a Total Exchange Flow (TEF) methodology (Ganju et al., 2012).

5.2. Biogeochemical model

The phytoplankton dynamics are simulated using a biogeochemical nutrient, phytoplankton, zooplankton, and detritus (NPZD) model (Fennel et al., 2006). This model is implemented into ROMS, and assumes nitrogen as the controlling nutrient for primary production. Therefore, it is based on the nitrogen cycle (Fig. 3), and includes the source, sink, and biogeochemical transformation terms of seven state variables: nitrate (NO_3), ammonium (NH_4), small and large detritus (SDet and LDet), phytoplankton (Phy), zooplankton (Zoo), and chlorophyll (Chl). We added the effect of seagrass nutrient uptake in order to account for its influence in nutrient cycling. This is represented in Fig. 3 by the arrow that goes from NH_4 to the sediment. We assumed that the uptake decreases with depth as seagrass biomass and production are strongly related with light availability (Cunningham, 2002). The mean nitrogen uptake by seagrasses in the bottom layer of the model varies between 0 and $10 \text{ mmolNm}^{-2}\text{day}^{-1}$ (Hemminga et al., 1991; Risgaard-Petersen et al., 1998; Hansen et al., 2000; Risgaard-Petersen and Ottosen, 2000), describing the nitrogen removal due to seagrass.

The main biogeochemical model equations were described by Fennel et al. (2006), who adapted them from the plankton dynamics model of Fasham et al. (1990). In the Fennel implementation, phytoplankton growth is a function of temperature, nutrient concentration, and the homogeneously integrated PAR distribution.

5.3. Irradiance model

Phytoplankton and seagrass growth are intrinsically dependent not only on light quantity but also on light quality. The basic irradiance formulation included in Fennel et al. (2006) did not account for spectral effects in considering light attenuation by water and chlorophyll. To better approximate light behavior, the spectral irradiance model used by Gallegos et al. (2011) was implemented. The atmospheric evolution of the spectral irradiance was formulated following Gregg and Carder (1990), which included

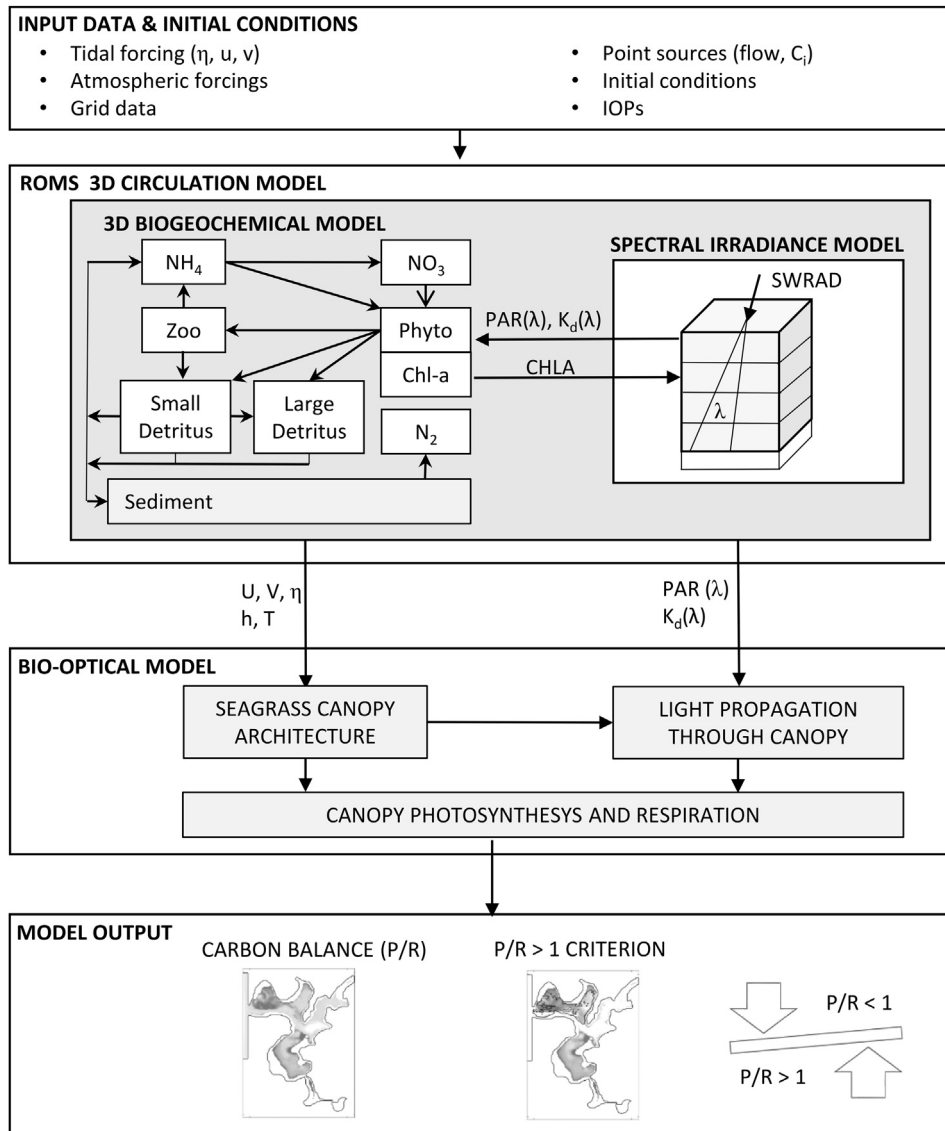


Fig. 3. Modeling system flowchart and interactions. In the bottom panel, P/R ratio >1 indicates potential seagrass habitat; P/R < 1 indicates potential loss of seagrass habitat. *U* and *V* are the velocities, *h* the water depth, *T* the water temperature and η the water surface variation.

absorption and scattering by ozone, oxygen, water vapor, and marine aerosols and also reflectance at the air-sea interface. In the current experiment, the observed PAR at the weather station was imposed at the water surface while enforcing the spectral shape given by the [Gregg and Carder \(1990\)](#) formulation for that time.

The implemented spectral attenuation in the water column from [Gallegos et al. \(2011\)](#) included the effects of water, CDOM, phytoplankton, and non-algal particulates (e.g., detritus, minerals, bacteria). In our simulations, the attenuation due to CDOM was assumed to be minimal because CDOM concentrations were negligible in the area under study (<3 QSU; <0.01 m⁻¹ absorbance at 400 nm). The water absorption and backscattering was assumed to follow the spectral characteristics of pure water. The light absorption and scattering by phytoplankton was represented as proportional to the chlorophyll-a concentration given by the [Fennel et al. \(2006\)](#) implementation. Meanwhile, the non-algal component of the spectral attenuation was taken as proportional to the total suspended solids concentration, which was considered constant in the present study. The spectral shape of the attenuation by each component followed the description in [Gallegos et al. \(2011\)](#). The

PAR distribution across the entire spectrum was integrated and used for the calculation of phytoplankton growth. The spectral PAR was used to determine seagrass growth as part of the [Zimmerman \(2003\)](#) bio-optical model.

5.4. Bio-optical seagrass model

We linked a bio-optical model ([Fig. 3](#)) to compute the carbon balance based on light conditions and photosynthesis. The model developed by [Zimmerman \(2003\)](#) consists of three different modules: a module that simulates the seagrass relative biomass and architecture including leaf geometry, an irradiance module that calculates the light absorption and scattering through the canopy, and a photosynthesis module that calculates the carbon balance (primary production and respiration) of the submerged plant canopy. The original 1D model simulates the light environment of a submerged canopy at a fixed horizontal point. However, we have applied the model to the entire domain. We have assumed initial seagrass presence in the entire system allowing the description of the light environment by dividing the canopy volume, including the

leaves and the water column, into a series of horizontal sections of finite thickness. The optical properties of each section are based on the architecture of the canopy, the orientation and optical properties of the leaves, and the optical properties of the dissolved materials and suspended particles in the water column. Given the spectral PAR at canopy height from the irradiance model, it computes the seagrass Photosynthetically Usable Radiation (PUR) by computing the spectral absorption and scattering of the downwelling and upwelling photosynthetically active irradiance through the seagrass canopy. Finally, the model calculates the canopy carbon balance, by computing the photosynthesis/respiration ratio. This ratio was used to assess the seagrass presence/absence and survival under different scenarios and conditions. The threshold of $P/R = 1$ was chosen, as both autotrophic and heterotrophic ecosystems tend to approach $P/R = 1$ over time (Giddings and Eddlemon, 1978). Moreover, as the ecosystem under study is autotrophic, we have assumed that $P/R > 1$ is associated with seagrass success and growth, while $P/R < 1$ leads to seagrass disappearance.

6. Model skill assessment

In the present section the assessments of the biogeochemical, irradiance and bio-optical models are described. The hydrodynamics and freshwater fluxes were assessed in a previous study (Ganju et al., 2012). During the calibration process, all model parameters were adjusted to match measured values. The indicators used to calibrate the biogeochemical, irradiance and bio-optical models were chlorophyll-a concentration, light attenuation coefficient, and seagrass presence/absence, respectively.

6.1. Biogeochemical and irradiance model assessment

The calibration of the biogeochemical and irradiance model was focused on the three sites where field measurements were obtained, each one representative of Outer, Snug and South, respectively. The values of the model parameters were chosen within the range found in the literature (Andersen et al., 1987; Taylor, 1988; Wroblewski, 1989; Taylor et al., 1991; Fasham, 1995; Geider et al., 1997; Leonard et al., 1999; Lima and Doney, 2004) to maximize the agreement between model results and field data (Table 3).

We achieved the highest skill by adjusting values for m_p , μ_0 , G_{\max} and m_z (Table 4). In Snug and Outer harbors, with regards to the chlorophyll-a concentration and the light attenuation coefficient we achieved a bias close to zero. The similarity between the standard deviations suggests that the model properly describes the variability of the system in those areas. By contrast, in South Cove the difference between modeled and observed chlorophyll is larger.

It is important to note that for the K_d calculation we only considered PAR values over the 84th percentile of the distribution, which corresponds to the hours of highest light incidence, usually around noon. These values were selected because when a beam of light impacts the water surface perpendicularly or with low angles measured from the vertical, most of the light penetrates the water column, and the scattering on the water surface is minimal. However, the larger the incident angle, the less light penetrates the water column and the less accurate the PAR measurements become. We have used PAR values during times when sunbeams impact the water surface with low incidence angles to minimize this effect.

6.2. Seagrass bio-optical model assessment

The calibrated parameters for the bio-optical model were the bending angle, the maximum canopy height, and the shoot density. The bending angle selected was 45° representing the average angle

Table 3

Main biogeochemical and irradiance model parameters and chosen value (adapted from Fennel et al. (2006)).

Symbol	Definition	Calibrated value	Units	Range
μ_0	Phytoplankton growth rate	3	d^{-1}	$0.62^* - 3.0^{\dagger}$
K_{NO_3}	Half-saturation concentration for uptake of NO_3	0.1	$Mmol\ N\ m^{-3}$	$0.007 - 1.5^{\ddagger}$
K_{NH_4}	Half-saturation concentration for uptake of NH_4	1.5	$Mmol\ N\ m^{-3}$	$0.007 - 1.5^{\ddagger}$
α	Initial slope of the P-I curve	0.13	$Mol\ C\ gChl^{-1}\ (Wm^{-2})^{-1}\ d^{-1}$	$0.007 - 0.13^{\S}$
G_{\max}	Maximum grazing rate	0.6	$(mmol\ N\ m^{-3})^{-1}\ d^{-1}$	$0.5^* - 1.0^{\parallel}$
K_p	Half-saturation concentration of phytoplankton ingestion	2	$(mmol\ N\ m^{-3})^2$	$0.56 - 3.5^{\ddagger}$
m_p	Phytoplankton mortality	0.05	d^{-1}	$0.05 - 0.2^{**}$
t	Aggregation parameter	0.005	$(mmol\ N\ m^{-3})^{-1}\ d^{-1}$	$0.005 - 0.1^{\ddagger}$
Θ_{\max}	Maximum chlorophyll to phytoplankton ratio	0.068	$mgChl\ mg\ C^{-1}$	$0.005 - 0.072^{\S}$
m_z	Zooplankton mortality	0.025	$(mmol\ N\ m^{-3})^{-1}\ d^{-1}$	$0.025 - 0.25^{\ddagger}$
R_{SD}	Remineralization rate of suspended detritus	0.03	d^{-1}	$0.01 - 0.25^{\dagger\dagger}$
R_{LD}	Remineralization rate of large detritus	0.01	d^{-1}	$0.01 - 0.25^{\dagger\dagger}$
N_{\max}	Maximum nitrification rate	0.05	d^{-1}	$0.05 - 0.1^{\ddagger}$

* (Taylor, 1988).

† (Andersen et al., 1987).

‡ (Lima and Doney, 2004).

§ (Geider et al., 1997).

¶ (Wroblewski, 1989).

|| (Fasham, 1995).

** (Taylor et al., 1991).

†† (Leonard et al., 1999).

over a tidal cycle, and the maximum canopy height was 1 m (Ackerman, 2002). The chosen density was 525 shoots/ m^2 ; the observed plant density varies between 300 and 800 shoots/ m^2 in Outer Harbor (McGlathery, Marino, Hayn, and Howarth unpublished). The spectral PAR comes from the irradiance model, and is propagated through the canopy to the seafloor. The seafloor absorbance and reflectance properties were also considered with the composition of the bottom being a mixture between mud (representing organic detritus) and sand. The reflected light was also propagated upward through the canopy, so the primary production was calculated with the total light absorbed. The potential habitat was evaluated as a function of the Photosynthesis/Respiration (P/R)

Table 4

Mean values of chlorophyll-a and K_d , standard deviation (Std), and bias for Outer, Snug and South Harbors. Field values of chlorophyll-a and K_d were obtained processing data from sensors deployed during summer 2012. Model results were obtained for the same time-period.

Site	Chlorophyll-a			K_d		
	Mean \pm Std model ($\mu g/L$)	Mean \pm Std field ($\mu g/L$)	BIAS ($\mu g/L$)	Mean \pm Std Model (1/m)	Mean \pm Std field (1/m)	BIAS (1/m)
Outer	6.9 ± 3.7	6.5 ± 2.8	0.41	0.45 ± 0.07	0.45 ± 0.30	-0.001
Snug	28 ± 12	28 ± 9.9	0.33	0.79 ± 0.19	0.86 ± 0.16	-0.077
South	6.3 ± 3.9	10 ± 9.3	-3.9	-	-	-

ratio distribution (Fig. 4a) obtained using the mean data of the entire summer. We have considered the P/R ratio obtained as representative of the season in the year under study. We assumed that for $P/R > 1$ there is seagrass growth, and therefore presence, delimiting this threshold as the potential seagrass in the estuary. However, for $P/R \leq 1$ we assumed conditions are unfavorable to seagrass presence (Fig. 4b) as growth would be limited, being respiration larger than photosynthesis in those areas. Based on this criterion, we have obtained an agreement of 73.39% between modeled and field presence/absence data, taking into account Outer and Snug Harbor (Fig. 4c), as in South Cove seagrass is thought to have disappeared due to hydrodynamic reasons, and not due to the light conditions as can be seen in Fig. 4b. Additionally, in Fig. 4 we can see that seagrass is not present in the shallower areas of the estuary. This is due to the wetting and drying effect simulated by the model and the subtidal behavior of *Zostera marina* imposed in the model. The seagrass distribution obtained by the selected P/R criterion (Fig. 4d) was in agreement with the critical depth distribution obtained applying the depth–limitation equation proposed by Duarte et al. (2007).

7. Nitrate loading and sea-level rise scenarios

The coupled modeling system was applied to West Falmouth Harbor to assess the effects of nitrate reduction and sea-level rise on potential seagrass habitat during the summer. The simulations time period was of two months corresponding with July and August. Different nitrate loading and sea-level rise scenarios were

Table 5

Nitrate reduction and sea level rise scenarios. CS_0/NR_0/SLR_2012 is the initial scenario and it is common for all the case studies.

Combined scenario (CS)	Nitrate reduction scenarios (NR)	Nitrate input load reduction (%)	Sea-level rise scenarios (SLR)	Sea level rise (m)
CS_0	NR_0	0	SLR_2012	0
CS_1	NR_10	10	SLR_2015	0.02
CS_2	NR_25	25	SLR_2022	0.0436
CS_3	NR_50	50	SLR_2037	0.09
CS_4	NR_75	75	SLR_2062	0.18
CS_5	NR_94	94	SLR_2112	0.35

conducted corresponding to anticipated future summer scenarios (Table 5). We implemented a gradual decrease of the nitrate input load and an increase in sea-level rise based on the IPCC predictions (IPCC, 2007) for the next one-hundred years.

First, we analyzed the effects of nitrate reduction (NR) and sea-level rise (SLR) separately, and then we have configured combined scenarios (CS) to evaluate the simultaneous effect of both parameters (Table 5; Fig. 5). Not surprisingly, our results support the idea that improvements in light conditions for seagrass, and consequently higher P/R ratios, are achieved with decreases in nitrate loading (Fig. 5). The results point to a potential recovery of seagrass in Snug Harbor area when nitrate loading is reduced by 50% (Fig. 5; NR 50). The P/R ratio improves considerably in Snug Harbor with a 75% nitrate reduction (NR 75). On the contrary, sea-level rise provokes a P/R ratio decline in areas where there is currently seagrass

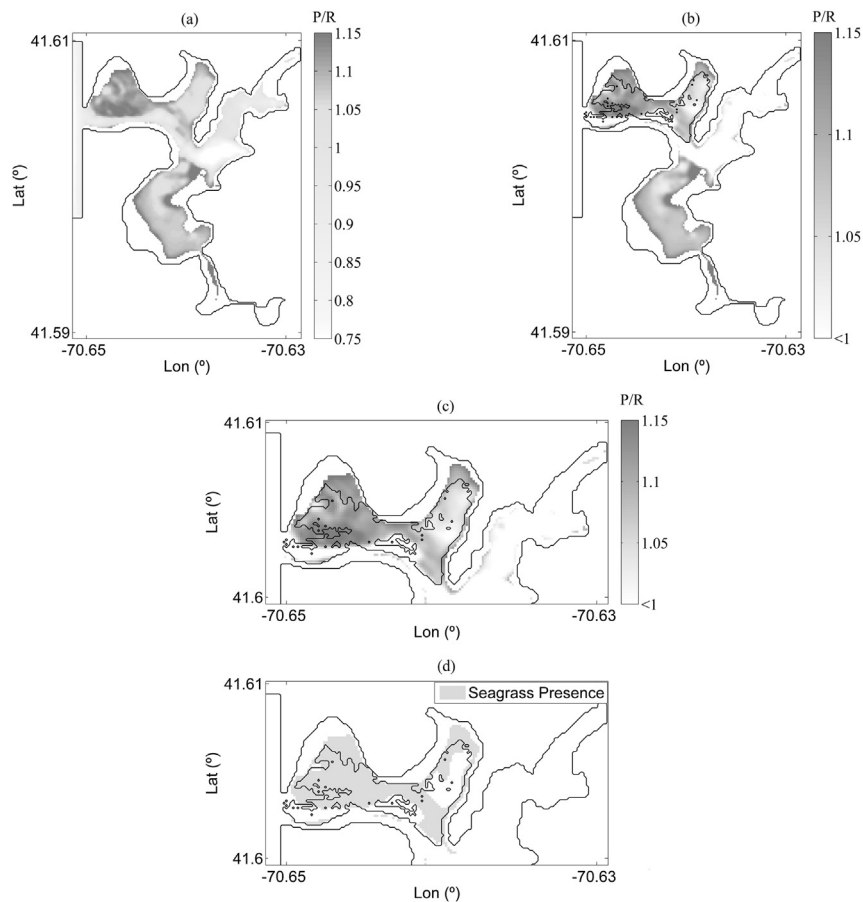


Fig. 4. a) Photosynthesis/Respiration ratio distribution; b) Photosynthesis/Respiration ratio distribution applying the $P/R > 1$ criterion and comparison with field data (black solid line); c) Detail of Snug and Outer P/R distribution with $P/R > 1$, and comparison with field data (black solid line); d) Seagrass distribution obtained with the depth-limited equation (Duarte et al., 2007). The white area represents where seagrass presence is discouraged ($P/R < 1$), the gray area the potential seagrass habitat ($P/R > 1$), and the black solid line delimits the seagrass presence area measured in the field survey.

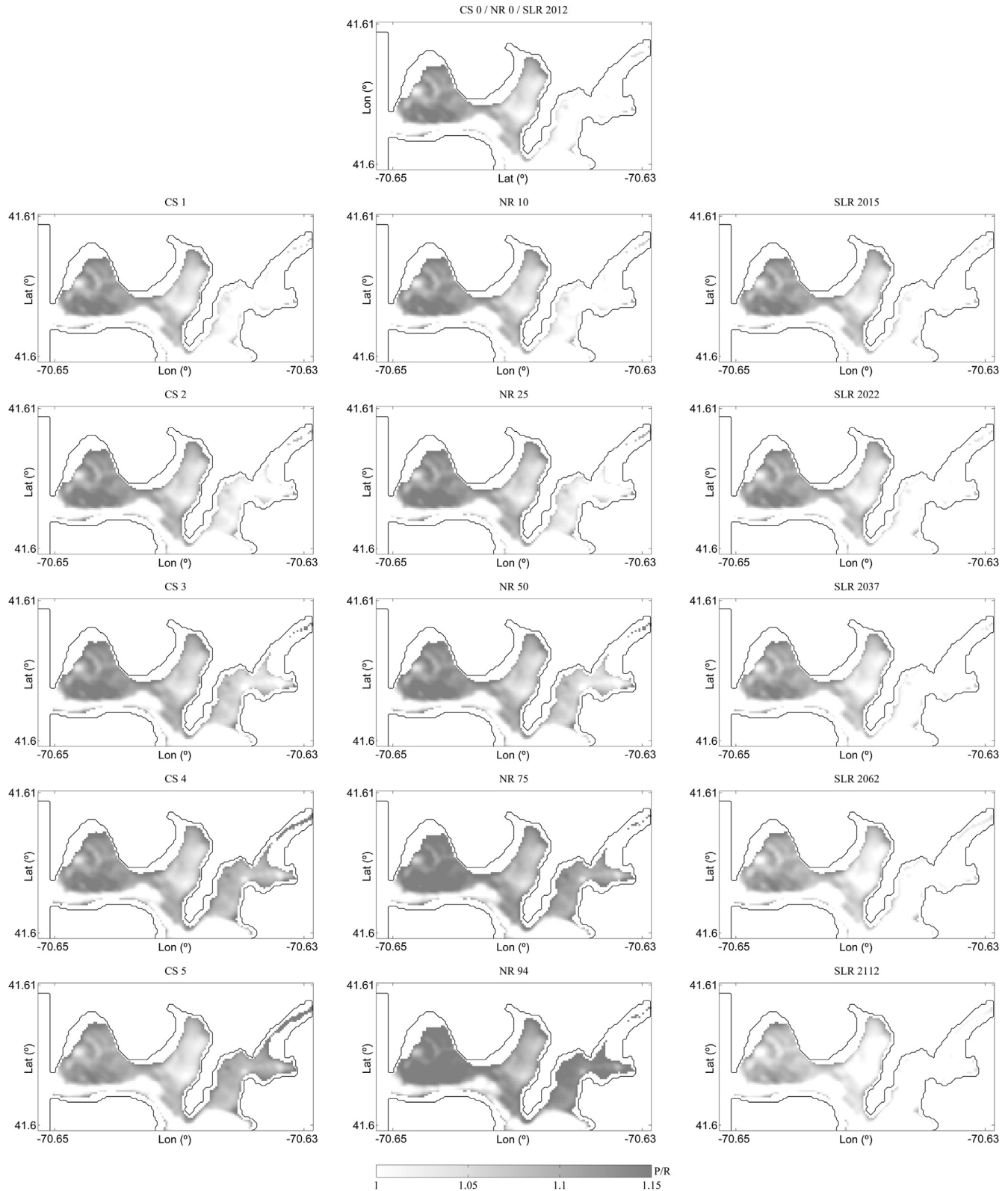


Fig. 5. Nitrate reduction (NR), sea-level rise (SLR) and combined (CS) scenarios. See Table 5 for an explanation of the scenarios nomenclature.

presence, as can be seen in SLR 2112. However, when both effects (SLR and NR) were studied together, a clear relationship between their combined behavior (CS) and the system response to nitrate reduction (NR) was observed. Hence, although sea-level rise increases water level and reduces light penetration, the light

attenuation change is not as significant as the nitrate loading effect. This is evident from comparing the temporal variation of P/R due to SLR vs. nitrate loading (Fig. 6). In Snug, the Figure shows a variation of P/R from 0.97 to 1.14 due to nitrate reduction, whereas light attenuation due to sea-level rise decreases P/R from 0.97 to 0.94. A

similar effect, due to sea-level rise, can be observed in Outer, with a P/R variation from 1.05 to 1.01 (Fig. 6). However, the nitrate reduction effect is lower in Outer, ranging from 1.05 to 1.10, due to the lower chlorophyll-a levels at this point. Moreover, the combined effect of sea-level rise and nutrient reduction led to a significant decrease of chlorophyll-a concentration and K_d , especially in Snug Harbor, with a reduction from $27.77 \mu\text{g L}^{-1}$ to $2.79 \mu\text{g L}^{-1}$ and 0.79 m^{-1} to 0.36 m^{-1} respectively (Fig. 7). Consequently, P/R in Snug Harbor increases from 0.97 to 1.09, providing adequate conditions for seagrass growth past CS_3. P/R in Outer Harbor slightly increased until CS_4, where it reached a maximum value of 1.07, and decreased to 1.05 in CS_5 due to sea-level rise influence. We have also obtained the evolution of potential seagrass area on the estuary for the different combined scenarios (Fig. 7). We obtained an 8% increase at CS_1, having an accumulated growth of 21% and 34% at CS_2 and CS_3 respectively. In the case of CS_4 and CS_5 the influence of sea level rise makes the evolution slower, obtaining an area increase from CS_4 to CS_5 of only 3%, having CS_5 an accumulated area growth of 45% with respect to the original scenario (CS_0). Therefore, our results show that in this system, potential reductions in nitrate loading will be more important than sea-level rise. However, in other systems with low nitrate loading, sea-level rise may be more relevant.

8. Discussion

Phytoplankton bloom intensity can significantly depress the light climate in the bottom of the water column, and therefore, light sensitive biogeochemical processes such as photosynthesis and

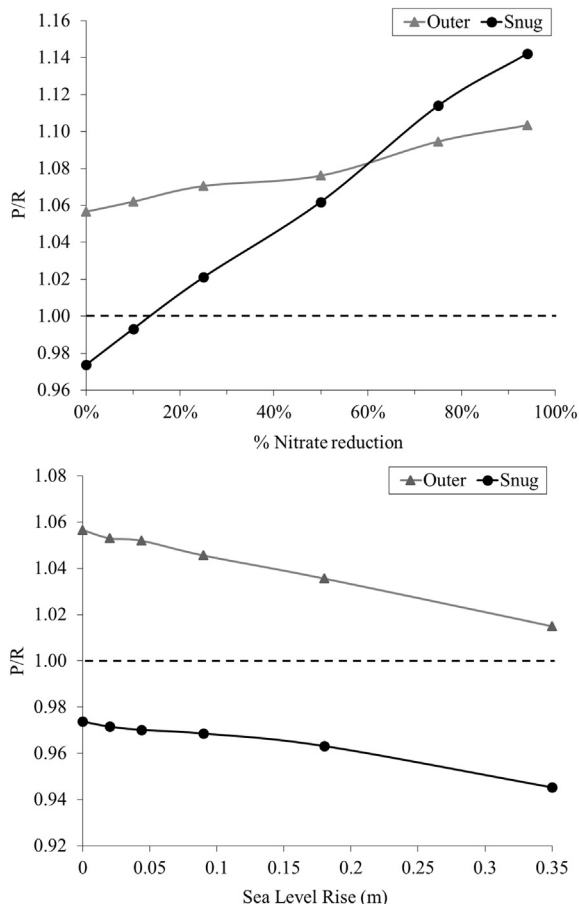


Fig. 6. P/R variation due to nitrate reduction and sea-level rise.

photo-oxidation. This has significant effects on seagrass distribution, as light is one of the main factors for seagrass growth and primary production. Our results support the idea that when insufficient light reaches the canopy seagrass presence diminishes, which is in agreement with previous studies (e.g. Dennison, 1987; Orth and Moore, 1988; Duarte, 1991; Duarte et al., 2007). Additionally, although there are relatively few known examples of seagrass meadow recovery following nitrate reductions (Burkholder et al., 2007) our results suggest that with progressive nitrate removal, Snug Harbor may recover from strictly a light perspective. Other factors such as macroalgae competition and morphodynamic changes should also be taken into account. For example, in South Cove, effects like competition with opportunistic macroalgae or seagrass death due to natural disturbances should be studied. However, the potential recovery of seagrass in Snug Harbor could be achieved due to the fact that the anthropogenic pressures that affect that area mainly consist of nitrate loading while macroalgal coverage is minimal. Nevertheless, the future effects of nitrate reduction in West Falmouth Harbor are hard to predict or evaluate with conventional techniques, as the transit time of the enriched water in the aquifer to the estuary is as much as 10 years (Kroeger et al., 2006). Moreover, we also obtained that nutrient concentration and therefore eutrophication are the processes that control seagrass distribution in the studied semienclosed microtidal shallow estuary, due to the light attenuation produced by them, which is in agreement with Burkholder et al. (2007) and Costa (1988). However, although seagrass distribution is strongly sensitive to light attenuation, it is also affected by other factors such as hypoxia, epiphyte growth, grazing, and hydrodynamic feedback, which are not included in this model as it has some limitations. However, further work will include these formulations. One of the factors that will also be considered in the modeling system is anoxia due to eutrophication, as the plant oxygen content is strongly dependent on photosynthesis and respiration (Greve et al., 2003), which have been computed in the model as a function of light and temperature. In fact, low oxygen levels could cause anoxia in the meristem that could also limit seagrass growth and primary production. The maintenance of oxic conditions in meristematic and belowground tissues is important for support seagrass growth, nutrient uptake by roots, and translocation of nutrients between roots and leaves (Zimmerman and Alberte, 1996; Greve et al., 2003). We have also neglected the role of epiphytes. Epiphytes attenuate light and expand around leaves limiting uptake of oxygen, inorganic carbon, and nutrients (Hauxwell et al., 2001). It is also important to include the effect of grazers: small invertebrate grazers generally have minimal negative impacts on seagrass growth and biomass, and may have important positive functions by controlling epiphyte growth; however, large grazers can impact seagrass meadows significantly (Stoner et al., 1995). Moreover, although currents and wave action can play an important role in seagrass distribution, the interactions between hydrodynamics and seagrasses were considered negligible in the present study, as this estuary is microtidal with limited fetch. Most of the recent modeling advances with respect to seagrasses are based on flow motion (Maza et al., 2013), morphodynamic changes (Bouma et al., 2008), and particle trapping (Hendriks et al., 2008). However, our modeling approach resolves the spatial pattern of seagrass habitat quality from a light perspective. In contrast to most of the existing ecological models, our coupled implementation computes spatially varying spectral light attenuation as a function of different attenuating substances with high vertical and horizontal discretization, allowing for delineation of the light climate for seagrass meadows. Moreover, as the irradiance model has been integrated into ROMS, which is an open-source flexible modeling system, our technique could be used in a wide range of applications. Moreover, the

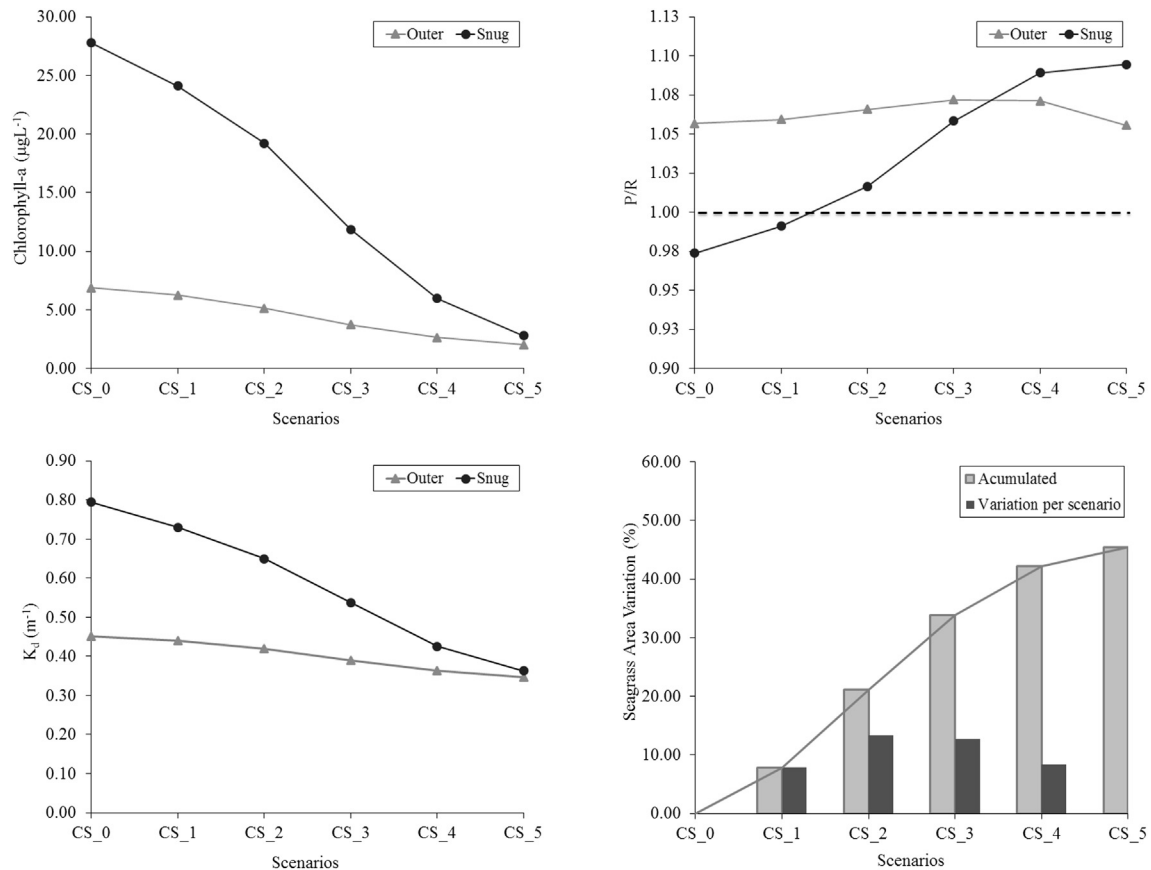


Fig. 7. Chlorophyll, K_d , P/R and seagrass area variation for the combined scenarios (CS). See Table 5 for an explanation of the scenarios nomenclature.

simplicity of its formulation makes it a non-high data demanding tool that is able to easily compute interpretable results. For example, the influence of sediment re-suspension and of the horizontal sediment transport on light availability could be assessed with this tool. Another possible application would be to analyze light climate variations due to spatial changes in CDOM caused by rivers flows, terrestrial runoff and/or microbial processes. This is possible due to the fact that ROMS is coupled to the Community Sediment Transport Modeling System (CSTMS) so the dynamical interaction between sediments and light availability can be modeled with this implementation.

9. Conclusions

In the present study, we have developed an approach to assess the potential recovery of seagrass communities under future nitrate loading and sea-level rise scenarios from a light perspective. We have assessed the model in a shallow temperate estuary, and capture the spatial variability of chlorophyll-a, light attenuation, and seagrass presence/absence. The coupled implementation computes spectral light attenuation as a function of different attenuating substances with high vertical and horizontal resolution, which allows the accurate determination of the light climate in the seagrass meadow. We find that, in general, increased sea-level will reduce light availability and is expected to negatively impact seagrasses, with a 11.4% reduction in presence/absence area with a 0.35 m increase in sea level. However, in the estuary studied here, reduction of nitrate loading is a larger factor in improvement of light availability. Seagrass habitat is expanded by 42.3% with a 94% reduction in nitrate loading. This study contributes to existing modeling

efforts by providing a new linked implementation for assessing seagrass potential habitat in terms of light availability. Future work should incorporate other ecological communities (macroalgae, epiphytes, grazers) as well as the effects of oxygen stress and hydrodynamic drag caused by vegetation.

Acknowledgments

This study was partially funded through a doctoral grant from the University of Cantabria and the Cantabria Government (BOC 25/01/2010). We also would like to thank Sophia Fox, Kevin Kroeger, Mark Brush, Renee Takesue, Javier García and Ivan Valiela, who provided helpful feedback in this study. Thanks also to Jonathan Borden, Kihoto Gitonga and Joseph Bergeron, who performed the field surveys, and to Eli Perrone and CR Environmental Inc. for assistance in conducting the sonar survey. Thanks to Richard C. Zimmerman and Charles L. Gallegos for providing the source code of their models, and to Sonia Castanedo, Giovanni Coco, Maitane Olabarrieta and Raúl Medina for their collaboration and support. Any use of trade, product, or firm names is for descriptive purposes only and does not imply endorsement by the U.S. Government.

References

- Ackerman, J.D., 2002. Diffusivity in a marine macrophyte canopy: implications for submarine pollination and dispersal. *Am. J. Bot.* 89, 1119–1127.
- Andersen, V., Nival, P., Harris, R.P., 1987. Modelling of a planktonic ecosystem in an enclosed water column. *J. - Mar. Biol. Assoc.* 67, 407–430.
- Bissett, W.P., Carder, K.L., Walsh, J.J., Dieterle, D.A., 1999a. Carbon cycling in the upper waters of the Sargasso Sea: II. Numerical simulation of apparent and inherent optical properties. *Deep-Sea Res. Part Oceanogr. Res. Pap.* 46, 271–317.

- Bissett, W.P., Walsh, J.J., Dieterle, D.A., Carder, K.L., 1999b. Carbon cycling in the upper waters of the Sargasso Sea: I. Numerical simulation of differential carbon and nitrogen fluxes. *Deep-Sea Res. Part Oceanogr. Res. Pap.* 46, 205–269.
- Bouma, T.J., Friedrichs, M., Van Wesenbeeck, B.K., Brun, F.G., Temmerman, S., De Vries, M.B., Graf, G., Herman, P.M.J., 2008. Plant growth strategies directly affect biogeomorphology of estuaries. In: *River, Coastal and Estuarine Morphodynamics: RCEM 2007*, pp. 285–292.
- Burkholder, J.M., Tomasko, D.A., Touchette, B.W., 2007. Seagrasses and eutrophication. *J. Exp. Mar. Biol. Ecol.* 350, 46–72.
- Cabello-Pasini, A., Muñoz-Salazar, R., Ward, D.H., 2003. Annual variations of biomass and photosynthesis in *Zostera marina* at its southern end of distribution in the North Pacific. *Aquat. Bot.* 76, 31–47.
- Costa, J.E., 1988. Eelgrass in Buzzards Bay: Distribution, Production and Historical Changes in Abundance. United States Environmental Protection Agency, Boston, Massachusetts, p. 223.
- Costello, C.T., Kenworthy, W.J., 2011. Twelve-year mapping and change analysis of eelgrass (*Zostera marina*) areal abundance in Massachusetts (USA) identifies statewide declines. *Estuaries Coasts* 34, 232–242.
- Cunningham, I., 2002. Modelling Nitrogen Fluxes in Seagrass. The University of Western Australia.
- Dennison, W.C., 1987. Effects of light on seagrass photosynthesis, growth and depth distribution. *Aquat. Bot.* 27, 15–26.
- Dennison, W.C., Orth, R.J., Moore, K.A., Stevenson, J.C., Carter, V., Kollar, S., Bergstrom, P.W., Batiuk, R.A., 1993. Assessing water quality with submersed aquatic vegetation. *BioScience* 43, 86–94.
- Duarte, C.M., 1991. Seagrass depth limits. *Aquat. Bot.* 40, 363–377.
- Duarte, C.M., Marba, N., Krause-Jensen, D., Sánchez-Camacho, M., 2007. Testing the predictive power of seagrass depth limit models. *Estuaries Coasts* 30, 652–656.
- Everett, J.D., Baird, M.E., Suthers, I.M., 2007. Nutrient and plankton dynamics in an intermittently closed/open lagoon, Smiths Lake, south-eastern Australia: an ecological model. *Estuar. Coast. Shelf Sci.* 72, 690–702.
- Fasham, M.J., 1995. Variations in the seasonal cycle of biological production in subarctic oceans: a model sensitivity analysis. *Deep-Sea Res. Part Oceanogr. Res. Pap.* 42, 1111–1149.
- Fasham, M.J.R., Ducklow, H.W., McKelvie, S.M., 1990. A nitrogen-based model of plankton dynamics in the oceanic mixed layer. *J. Mar. Res.* 48, 591–639.
- Fennel, K., Wilkin, J., Levin, J., Moisan, J., O'Reilly, J., Haidvogel, D., 2006. Nitrogen cycling in the Middle Atlantic Bight: results from a three-dimensional model and implications for the North Atlantic nitrogen budget. *Glob. Biogeochem. Cycles* 20.
- Gallegos, C.L., Werdell, P.J., McClain, C.R., 2011. Long-term changes in light scattering in Chesapeake Bay inferred from Secchi depth, light attenuation, and remote sensing measurements. *J. Geophys. Res.* 116.
- Ganju, N., Dickhudt, P., Thomas, J., Borden, J., Sherwood, C., Montgomery, E., Twomey, E., Martini, M., 2011. Summary of Oceanographic and Water-quality Measurements in West Falmouth Harbor and Buzzards Bay, Massachusetts, 2009–2010. U.S. Geological Survey, Open-File Report 2011-1113. Also available at: <http://pubs.usgs.gov/of/2011/1113/> <http://pubs.usgs.gov/of/2011/1113/>.
- Ganju, N.K., Hayn, M., Chen, S.N., Howarth, R.W., Dickhudt, P.J., Aretxabaleta, A.L., Marino, R., 2012. Tidal and groundwater fluxes to a shallow, microtidal estuary: constraining inputs through field observations and hydrodynamic modeling. *Estuaries Coasts* 35, 1285–1298.
- Geider, R.J., MacIntyre, H.L., Kana, T.M., 1997. Dynamic model of phytoplankton growth and acclimation: responses of the balanced growth rate and the chlorophyll a:carbon ratio to light, nutrient-limitation and temperature. *Mar. Ecol. Prog. Ser.* 148, 187–200.
- Giddings, J., Eddlemon, G.K., 1978. Photosynthesis/respiration ratios in aquatic microcosms under arsenic stress. *Water, Air Soil. Pollut.* 9 (2), 207–212.
- Gregg, W.W., Carder, K.L., 1990. A simple spectral solar irradiance model for cloudless maritime atmospheres. *Limnol. Oceanogr.* 35, 1657–1675.
- Greve, T.M., Borum, J., Pedersen, O., 2003. Meristematic oxygen variability in eelgrass (*Zostera marina*). *Limnol. Oceanogr.* 48, 210–216.
- Haidvogel, D.B., Arango, H., Budgell, W.P., Cornuelle, B.D., Curchitser, E., Di Lorenzo, E., Fennel, K., Geyer, W.R., Hermann, A.J., Lanerolle, L., Levin, J., McWilliams, J.C., Miller, A.J., Moore, A.M., Powell, T.M., Shchepetkin, A.F., Sherwood, C.R., Signell, R.P., Warner, J.C., Wilkin, J., 2008. Ocean forecasting in terrain-following coordinates: formulation and skill assessment of the regional ocean modeling system. *J. Comput. Phys.* 227, 3595–3624.
- Hansen, J.W., Pedersen, A.-G.U., Bernsten, J., Ronbog, I.S., Hansen, L.S., Lomstein, B.A., 2000. Photosynthesis, respiration, and nitrogen uptake by different compartments of a *Zostera marina* community. *Aquat. Bot.* 66, 281–295.
- Hauxwell, J., Cebrian, J., Furlong, C., Valiela, I., 2001. Macroalgal canopies contribute to eelgrass (*Zostera Marina*) decline in temperate estuarine ecosystems. *Ecology* 82, 1007–1022.
- Hayn, M., Howarth, R., Marino, R., Ganju, N., Berg, P., Foreman, K., Giblin, A., 2014. Exchange of nitrogen and phosphorus between a shallow lagoon and coastal waters. *Estuaries Coasts* 37, S63–S73 (Suppl. 1).
- Hayn, M., 2012. Exchange of Nitrogen and Phosphorus between a Shallow Estuary and Coastal Waters. MS thesis. Department of Natural Resources, Cornell University, p. 73.
- Hemminga, M., Duarte, C., 2000. *Seagrass Ecology*. Cambridge University Press.
- Hemminga, M.A., Harrison, P.G., Van Lent, F., 1991. The balance of nutrient losses and gains in seagrass meadows. *Mar. Ecol. Prog. Ser.* 71, 85–96.
- Hendriks, I.E., Sintes, T., Bouma, T.J., Duarte, C.M., 2008. Experimental assessment and modeling evaluation of the effects of the seagrass *Posidonia oceanica* on flow and particle trapping. *Mar. Ecol. Prog. Ser.* 356, 163–173.
- Hipsey, M.R., Hamilton, D.P., 2008. *Computational Aquatic Ecosystem Dynamic Model: CAEDYM v3 Science Manual*. Centre for Water Research.
- Howarth, R.W., Hayn, M., Marino, R.M., Ganju, N., Foreman, K., McGlathery, K., Giblin, A.E., Berg, P., Walker, J.D., 2014. Metabolism of a nitrogen-enriched coastal marine lagoon during the summertime. *Biogeochemistry* 118, 1–20.
- Howes, B.L., Kelley, S.W., Ramsey, J.S., Samimy, R., Schlezinger, D., 2006. Linked Watershed-embayment Model to Determine Critical Nitrogen Loading Thresholds for West Falmouth Harbor, Falmouth, Massachusetts. Massachusetts Estuaries Project. Massachusetts Department of Environmental Protection, Boston, Massachusetts, p. 161.
- IPCC, 2007. *Climate change 2007: impacts, adaptation and vulnerability*. In: Parry, M.L., Canziani, O.F., Palutikof, J.P., van der Linden, P.J., Hanson, C.E. (Eds.), *Contribution of Working Group II to the Fourth Assessment Report of the Intergovernmental Panel on Climate Change*. Cambridge University Press, Cambridge, UK, p. 976.
- Kroeger, K.D., Cole, M.L., York, J.K., Valiela, I., 2006. Nitrogen loads to estuaries from waste water plumes: modeling and isotopic approaches. *Ground Water* 44, 188–200.
- Lee, K.S., Park, S.R., Kim, Y.K., 2007. Effects of irradiance, temperature, and nutrients on growth dynamics of seagrasses: a review. *J. Exp. Mar. Biol. Ecol.* 350, 144–175.
- Leonard, C.L., McClain, C.R., Murtugudde, R., Hofmann, E.E., Harding Jr., L.W., 1999. An iron-based ecosystem model of the central equatorial Pacific. *J. Geophys. Res. C: Oceans* 104, 1325–1341.
- Lima, I.D., Doney, S.C., 2004. A three-dimensional, multnutrient, and size-structured ecosystem model for the North Atlantic. *GB3019 Glob. Biogeochem. Cycles* 18, 3011–3021.
- Marchesiello, P., McWilliams, J.C., Shchepetkin, A., 2003. Equilibrium structure and dynamics of the California current system. *J. Phys. Oceanogr.* 33, 753–783.
- Maza, M., Lara, J.L., Losada, I.J., 2013. A coupled model of submerged vegetation under oscillatory flow using Navier–Stokes equations. *Coast. Eng.* 80, 16–34.
- McGlathery, K.J., Sundback, K., Anderson, I.C., 2007. Eutrophication in shallow coastal bays and lagoons: the role of plants in the coastal filter. *Mar. Ecol. Prog. Ser.* 348, 1–18.
- Nixon, S.W., Buckley, B., Granger, S., Bintz, J., 2001. Responses of very shallow marine ecosystems to nutrient enrichment. *Hum. Ecol. Risk Assess.* 7, 1457–1481.
- Orth, R.J., Moore, K.A., 1988. Distribution of *Zostera marina* L. and *Ruppia maritima* L. sensu lato along depth gradients in the lower Chesapeake Bay, U.S.A. *Aquat. Bot.* 32, 291–305.
- Orth, R.J., Carruthers, T.J.B., Dennison, W.C., Duarte, C.M., Fourqurean, J.W., Heck Jr., K.L., Hughes, A.R., Kendrick, G.A., Kenworthy, W.J., Olyarnik, S., Short, F.T., Waycott, M., Williams, S.L., 2006. A global crisis for seagrass ecosystems. *BioScience* 56, 987–996.
- Risgaard-Petersen, N., Dalsgaard, T., Rysgaard, S., Christensen, P.B., Borum, J., McGlathery, K., Nielsen, L.P., 1998. Nitrogen balance of a temperate eelgrass *Zostera marina* bed. *Mar. Ecol. Prog. Ser.* 174, 281–291.
- Risgaard-Petersen, N., Ottosen, L.D.M., 2000. Nitrogen cycling in two temperate *Zostera marina* beds: seasonal variation. *Mar. Ecol. Prog. Ser.* 198, 93–107.
- Short, F.T., Neckles, H.A., 1999. The effects of global climate change on seagrasses. *Aquat. Bot.* 63, 169–196.
- Short, F.T., Wyllie-Echeverria, S., 1996. Natural and human-induced disturbance of seagrasses. *Environ. Conserv.* 23, 17–27.
- Short, F.T., Short, C.A., 2004. *Seagrasses of the Western North Atlantic*. In: Green, E.P., Short, F.T. (Eds.), *World Atlas of Seagrasses*. University of California Press, Berkeley, CA, pp. 207–215.
- Stoner, A.W., Ray, M., Waite, J.M., 1995. Effects of a large herbivorous gastropod on macro-fauna communities in tropical seagrass meadows. *Mar. Ecol. Prog. Ser.* 121, 125–137.
- Taylor, A.H., 1988. Characteristic properties of models for the vertical distribution of phytoplankton under stratification. *Ecol. Model.* 40, 175–199.
- Taylor, A.H., Watson, A.J., Ainsworth, M., Robertson, J.E., Turner, D.R., 1991. A modelling investigation of the role of phytoplankton in the balance of carbon at the surface of the North Atlantic. *Glob. Biogeochem. Cycles* 5, 151–171.
- Terrados, J., Borum, J., 2004. Why are seagrasses important?—Goods and services provided by seagrass meadows, 2006. In: Borum, J., Duarte, C.M., Krause-Jensen, D., Greve, T.M. (Eds.), *European Seagrasses: an Introduction to Monitoring and Management*, pp. 8–10, 88.
- Titus, J.G., Andreson, K.E., Cahoon, D.R., Gesch, D.B., Gill, S.K., Gutierrez, B.T., Thieler, E.R., Williams, S.J., 2009. Coastal Sensitivity to Sea-level Rise: a Focus on the Mid-Atlantic Region. U.S. Climate Change Science Program, p. 320.
- Waycott, M., Duarte, C.M., Carruthers, T.J.B., Orth, R.J., Dennison, W.C., Olyarnik, S., Calladine, A., Fourqurean, J.W., Heck Jr., K.L., Hughes, A.R., Kendrick, G.A., Kenworthy, W.J., Short, F.T., Williams, S.L., 2009. Accelerating loss of seagrasses across the globe threatens coastal ecosystems. *Proc. Natl. Acad. Sci. U. S. A.* 106, 12377–12381.
- Wroblewski, J.S., 1989. A model of the spring bloom in the North Atlantic and its impact on ocean optics. *Limnol. Oceanogr.* 34, 1563–1571.
- Zimmerman, R.C., 2003. A biooptical model of irradiance distribution and photosynthesis in seagrass canopies. *Limnol. Oceanogr.* 48, 568–585.
- Zimmerman, R.C., Alberte, R.S., 1996. Effect of light/dark transition on carbon translocation in eelgrass *Zostera marina* seedlings. *Mar. Ecol. Prog. Ser.* 136, 305–309.